Preliminary Study of Direct High-Temperature Air Generation Inside Linear Fresnel Concentrating Solar Collectors

Antonio Famiglietti[1], Antonio Lecuona-Neumann[1], Mohammad Rahjoo[1], José Nogueira-Goriba[1]

[1] Grupo ITEA. Departamento de Ingeniería Térmica y de Fluidos, Universidad Carlos III de Madrid, Avda. de la Universidad 30, 28911 Leganés, Madrid, (Spain)

Abstract

Medium temperature heat required by industry and food processing facilities worldwide is provided mainly consuming fossil fuel. Alternative renewable energy sources are needed to reduce the environmental impact of high energy-demanding sectors and prevent fuel scarcity. Among solar technologies, concentrating collectors enable to provide high and medium temperature heat, showing great potential as an alternative energy source.

In order to reduce the complexity and cost of the solar facility, a novel layout is proposed in this work, aiming at the feasibility of direct air heating inside a linear concentrating collector. The drawback of modest air heat capacity is mitigated by increasing the density and recovering the compression power through a turbine. It results in a special solar Brayton cycle, aiming to produce medium temperature air instead of mechanical power. This paper proposes a model for the dimensioning of facilities and estimation of their performances.

Direct Air Heating, SHIP, Solar Heat for Industry, Linear Fresnel collectors, Brayton cycle

1. Introduction

According to (European Comission, 2018) heating and cooling today, represent 46% of the EU energy system. The EU industry uses 70.6% of the energy consumption (193.6 Mtoe) for space and industrial process heating and around 50% of the energy consumption by industry is used for producing heat below 400 ºC, (IRENA, 2015). In the medium temperature heat range (200 ºC to 400 ºC) a wide range of processes use air as heat carrier, some applications are food processing, residual wastewater sludge drying and conditioning, painted products curing, thermal treatment of different wood base materials, ceramics, mining products, plastic and rubber treatment to grains, seeds, and biomass (Farjana, Huda, Parvez Mahmud, & Saidur, 2018). Linear concentrating solar collectors, either parabolic trough PTC or linear Fresnel LFC types, are suitable for providing heat up to 400°C, so that they are receiving growing attention as renewable energy source for industrial processes in the medium temperature range. The wide range of industrial processes using hot air and the capability of linear concentrating collectors for providing medium temperature heat, suggest to explore the feasibility of direct air heating inside the solar receiver tube. Eliminating a dedicated heat transfer fluid HTF, usually, a technical liquid and the associated liquid/air heat exchanger results in an open circuit heating system, using only ambient air as Heat Transfer Fluid HTF. Using air as HTF offers lower cost, lower weight, and simplicity. Also, it offers reduced risks associated with leakages, no need for antifreeze or thermal oil and reduced maintenance costs. In spite of these advantages, direct air heating inside PTC or LFC is not a common practice due to physical air properties. In fact, low density, low thermal conductivity and low heat capacity can lead to a poor internal heat transfer as well as high flow velocity inside the receiver tube. As consequence high pumping power is required for air circulation in order to avoid tube overheating. This issue is explained in Section 2. The drawbacks of using air can be overcome using a turbocharger to boost air pumping, configuring a turbo-assisted solar air heater, presented in Section 3. In Section 4 main numerical results, concerning the feasibility analysis of the proposed technology, are presented.

doi:10.18086/swc.2019.12.04 Available at http://proceedings.ises.org

2. Direct air heating

Linear concentrating solar collectors, either linear Fresnel LFCs, or parabolic trough collectors PTCs, are receiving growing attention as an available technology for solar heat production for industrial applications, both for their economic cost and the capability to produce high temperatures. In common practice, a liquid Heat Transfer Fluid HTF, carries solar heat from the receiver tube to a heat exchanger HX, which deliver it to the thermal process, as in a closed-loop layout in Fig.1. HTF, such as thermal oil, molten salt or pressurized water are generally used for this purpose, introducing several drawbacks, such as risk of hot liquid leakages, thermal degradation, fire hazards, and corrosion. The HTF and the HX strongly affect the total cost of the solar facility.

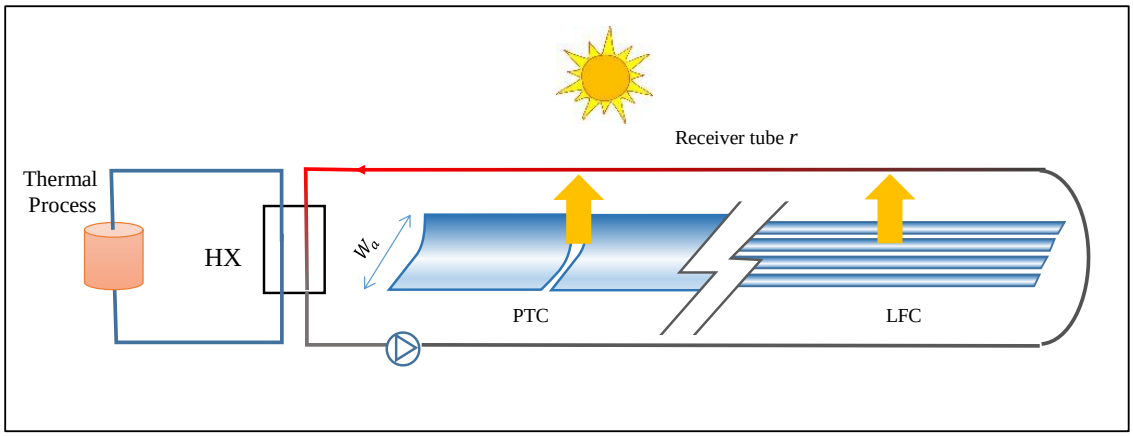

Fig 1. Common layout of solar heating for industrial process using PTC or LFC.

A wide variety of industrial processes that are in the midst of moderate temperatures suggest that the feasibility of directly heating air inside the concentrating solar collector receiver tubes increases the safety, efficiency, and reduce the complexity.

The low specific heat capacity c_p of gaseous HTF compared with liquid substance is one of the main obstacles for the implementation of them in concentrating solar collectors. For usual densities, in order to achieve the proper heat capacity rate $\dot{m}c_p$ able to absorb the useful incoming solar power $\dot{Q}_u$ with an acceptable total static end temperature T_{ou}, a high average flow velocity v_m is required inside the receiver tube of diameter D, as stated in Eq.1, where the last term is usually negligible in front of solar heating.

$$T_{ou} = T_{int} + \frac{\dot{Q}_u}{c_p \underbrace{\rho_m \frac{D^2}{4} \pi v_m}_{\dot{m}}} - \frac{v_{ou}^2}{2c_p} \qquad \text{(eq.1)}$$

This results in a high stagnation pressure drop Δp_t inside the tube. Considering a receiver tube length L_t, the stagnation pressure drop Δp_t can be expressed assuming an incompressible average $_m$ flow for simplicity, as in Eq. 1. Friction factor f for $Re \gg 1$ can be estimated following (Blasius, 1913).

$$\Delta p_t = \frac{1}{2}\rho_m v_m^2 f \frac{L_t}{D} = \frac{1}{2}\rho_m v_m^2 \underbrace{\left(0.316 Re_{D,m}^{-\frac{1}{4}}\right)}_{f} \frac{L_t}{D} \qquad \text{(eq.2)}$$

As a consequence of the high velocity, the pumping power $\dot{W}_p = \Delta p_t \dot{m} \rho_m^{-1}$ required to drive the gas through the

tube can be remarkable, resulting in excessive electricity consumption. Eq.3 defines $\dot{W}_p$. Introducing Eq.2 in Eq.3, the dependency of $\dot{W}_p$ on the average flow magnitudes can be obtained, as follows.

$$\dot{W}_p = \frac{\Delta p_t \dot{m}}{\rho_m} = \frac{1}{2} v_m^2 f \frac{L_t}{D} \dot{m} = v_m^2 f \frac{L_t}{D} \left(\rho_m v_m \frac{\pi D^2}{4} \right) \sim 0.04 \pi L_t D^{0.75} (\rho^{0.75} \mu^{0.25} \nu^{2.75})_m \quad \text{(eq.3)}$$

For a given tube diameter, limited to commercial standards for evacuated solar receiver tubes, $\dot{W}_p$ increases with collector length L_t due to a larger friction surface. On the other hand, longer collector rows as well as wider aperture widths L_a increase the gathered incoming solar power $\dot{Q}_u$ so that higher mass flow rates must be used to limit the outlet tube temperature T_{ou}, leading to higher mean velocities, as in Eq.1. As a consequence, $\dot{W}_p$ can be high, even reaching the same order of magnitude of incoming solar power, for medium and large installations.

The large pumping power consumption can affect the feasibility of direct air heating, although this is not the only drawback. In fact, besides to thermal capacity rate, the physical air properties also affect the heat transfer occurring between the irradiated tube surface and the internal gas flow. The Dittus-Boelter expression for wall-to-air heat transfer coefficient h , indicated in Eq.4, gives a reasonable accuracy for the purpose.

$$h = \frac{k}{D} 0.023 Re_{Dm}^{0.8} Pr^{0.4} \quad \text{eq.(4)}$$

Owing to the low thermal conductivity k and low specific heat capacity c_p of air, internal heat transfer is modest, thus inducing higher wall over-temperature $\Delta T_w = T_w - T_{ou}$ with respect to a liquid HTF application, as in Eq. 5. This is critical at the outlet of the tube row, where the fluid temperature is maximum T_{ou}. Actually ΔT_w can be in the same order of magnitude of the temperature rise $\Delta T = T_{ou} - T_{in}$. An excessively high wall temperature T_w can overcome the solar receiver thermal limit $T_{w,max}$.

$$\Delta T_w = T_w - T_{ou} = \frac{\dot{q}_u}{h} = \frac{\dot{q}_u D}{k 0.023 Re_{D,ou}^{0.8} P_r^{0.4}} = \left(\frac{\dot{q}_u D^{0.2} \mu^{0.4}}{0.023\, c_p^{0.4} \nu^{0.8} \rho^{0.8} k^{0.6}} \right)_{ou} \quad \text{(eq.5)}$$

3. Proposal description

The innovative layout proposed here, already patented (Spain Patent No. P201630068, 2016), aims to alleviate the drawbacks of gaseous HTF through the implementation of a turbocharger. As stated in Eq. 3, pumping power is strongly dependent on flow velocity. For a given mass flow rate $\dot{m}$, needed according to solar power to limit end air temperature T_{ou} as well as T_w, an increase in density results in lower mean velocity, diminishing the pumping power. For that purpose, a compressor c is introduced to increase the air density before pumping it through the solar receiver r, in Fig.2. Besides that, recovering the compressing and pumping power with a turbine e can bring the possibility of working with higher mass flow rates to limit the wall temperature, thus protecting the receiver optically selective surface. This layout configures an open circuit Brayton cycle, its main purpose is to provide a medium temperature airflow after expansion, instead of converting heat into mechanical power at the turbocharger shaft, Fig.2. Direct solar air heating without external power consumption is achieved as the turbine drives the compressor after solar heating.

Solar Brayton cycle have been studied by several authors with different purposes of the present proposal. (Bellos, Tzivanidis, & Antonopoulos, 2017) and (Cinocca, Cipollone, Carapellucci, Iampieri, & Mattia, 2018) among others studied the use of concentrating solar collectors in a Brayton cycle for power generation. High temperature $\sim 1000°C$ required by a Brayton cycle for efficient power production (Wilson & Korakianitis, 1998), it can not be reached inside linear concentrating collector, due to lower thermal limit of the solar receiver tube $\sim 600°C$ (Zhu, Wendelin, Wagner, & Kutscher, 2014). For that a combustion chamber or a post-heating unit is needed for further increase temperature, while the solar collector are used for air pre-heating, reducing fuel consumption.

The layout presented here aim to use only solar energy source to run special Brayton cycle with null efficiency, in

order to produce heat instead of power. Solar thermal energy provides the pumping power required for air circulation inside the system and eventually up to user process. Hot air can be provided at moderate overpressure above the atmospheric condition, which can be beneficial for the user thermal processes. For this purpose an turbocharger is used, which is cheap and well known technology developed for internal combustion engines industry.

Although the concept is more suitable for medium and large installation, it is applied here to a small scale linear Fresnel collector LFC in order to evaluated the feasibility of prototype scale facility. The general analysis can be extended to parabolic trough collector PTC as well.

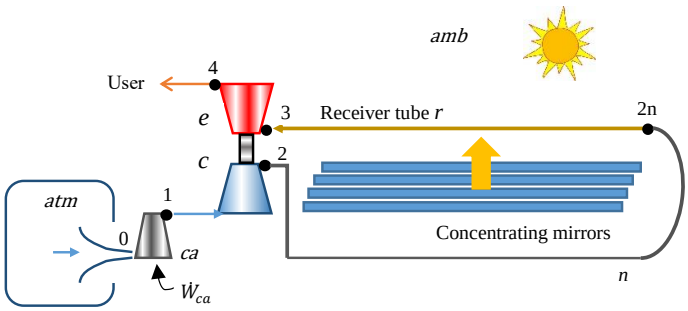

Fig. 2: General layout

A general model of the proposed layout is developed using the following equations. The auxiliary compressor ca in Fig.2 is excluded from the circuit during steady operation, being only needed during starting transient, so it does not appear in the following model. Ambient air is compressed by compressor c up to total pressure $p_{2t} = p_{0t}\pi_c$. With a total to total isoentropic efficiency η_{ctt} and a total to total pressure ratio π_c, the compressor consumes a mechanical power $\dot{W}_c$, (Balje, 1981):

$$\dot{W}_c = \left(\pi_c^{\frac{\gamma_c-1}{\gamma_c}} - 1\right)\eta_{ctt}^{-1}\dot{m}\bar{c}_{pc}T_{0t}\ ;\ T_{0t} = T_{atm} \qquad \text{Eq.(6)}$$

The compressor feeds air to the receiver tube trough a connection pipe n. Thermal losses in pipe n, supposed to be thermally isolated, are negligible so that air enters the collector a temperature T_{in}, Eq.7.

$$T_{in} = T_{2n} = T_2 = T_{0t}\left[1 + \left(\pi_c^{\frac{\gamma_c-1}{\gamma_c}} - 1\right)\eta_{ctt}^{-1}\right] - \frac{{v_2}^2}{2c_{p2}} \qquad \text{Eq.(7)}$$

Air heating inside the receiver results from the power balance over the tube length L_t. According to the simplified approach chosen, the solar power available at the receiver tube surface is estimated as $\dot{Q}_s = W_a L_t G_{bn}\eta_{op}$ as a first approximation, resulting from the concentrating effect of the linear Fresnel collector of length L_t and aperture width W_a. G_{bn} is the normal direct beam irradiance impacting on the aperture area $A_a = W_a L_t$. A detailed model of Fresnel concentrator to determine the optical efficiency $\eta_{op} = \eta_{op,max}IAM$ is out of the scope of this work, according to simplified approach adopted in the preliminary viability study. Optical efficiency model of LFC involves a maximum constant efficiency $\eta_{op,max}$, which is characteristic of the collector design and manufacturing, and several effects dependent on solar incident angle, accounted by an incident angle modifier IAM. Cosine effect, mirrors mutual shadowing, blocking, shadowing of secondary optics, as well as end optical losses must be taken into account for determining IAM . Mentioned effects are generally separated into transversal and longitudinal effects, accounted by IAM_L and IAM_T and end losses accounted by a factor f_{end}, so that results $IAM = IAM_L IAM_T f_{end}$. IAM changes with sun position according to collector orientation and length. In order to hold general validity in this study $G_{bn}\eta_{op,max}IAM$ is considered as relevant input parameter, varying it in a reasonable range for viability evaluation.

The thermal losses to the ambient can be estimated considering an average wall-to-ambient heat transfer coefficient $\bar{U}_l$. According to the technical literature, for an evacuated tube equipped with selective coating a representative

value of $\bar{U}_l = 5\frac{\mathrm{W}}{\mathrm{m^2K}}$ is assumed in this study. Following (Duffie & Beckman, 1991) the incoming solar power delivered to the air flow $\dot{Q}_u$ can be expressed only in terms of the inlet temperature T_{in}, as in Eq. 8, introducing the collector efficiency factor F' and heat dissipation factor F_R, which consider constant parameters along L_t.

$$\dot{Q}_u = F_R L_t\left[W_a G_{bn}\eta_{op,max} IAM - P_{ex}\bar{U}_l(T_{in} - T_{amb})\right] = \dot{m}c_p(T_{out} - T_{int}) \quad \text{Eq.(8)}$$

$P_{ex} = D_{ex}\pi$ is the external tube perimeter. F_R and F' are defined as:

$$F_R = \frac{\dot{m}c_{pm}}{L_t P_{ex}\bar{U}_l}\left[1 - \exp\left(-\frac{F' L_t P_{ex}\bar{U}_l}{\dot{m}c_{pm}}\right)\right] \quad \text{Eq.(9)}$$

$$F' = \frac{\bar{U}_l^{-1}}{\bar{U}_l^{-1} + \frac{D_{ex}}{Dh} + \frac{D_{ex}\ln\left(\frac{D_{ex}}{D}\right)}{2k_r}} \cong \left(1 + \frac{D_{ex}\bar{U}_l}{Dh}\right)^{-1} \quad \text{Eq.(10)}$$

The outlet tube temperature $T_{ou} = T_3$ resulting from Eq.(8) corresponds to the inlet temperature for the turbine so that total temperature $T_{3t} = T_3 + {v_3}^2/2c_{p3}$ allows estimating the mechanical power extracted from the expanding air by the turbine, assuming a total to total isoentropic efficiency η_{ett} (Balje, 1981):

$$\dot{W}_e = T_{3t}\dot{m}\bar{c}_{pe}\left(1 - (p_{3t}/p_{4t})^{-\frac{\gamma_e - 1}{\gamma_e}}\right)\eta_{ett} \quad \text{Eq.(11)}$$

The inlet turbine pressure $p_{3t} = p_2 + \rho_3 {v_3}^2/2 - \Delta p_{nr}$ is affected by the pressure drops inside the pressurized circuit Δp_{nr}, including the pipe (*n* at Fig. 2, which carries air to the receiver) the receiver (*r* at Fig. 2), the bends and connections. $p_{4t} = p_{atm}\pi_R$ can be slightly higher than ambient pressure, depending on the turbine outlet diffuser. This eventuality is only possible if there is a continuing circuit to the user.

The turbine delivers air at medium temperature $T_4 = T_{4t} - \frac{{v_4}^2}{2c_{p,4}}$.

$$T_{4t} = T_{3t}\left[1 - \eta_{ett}(1 - (p_{3t}/p_{4t})^{-\frac{\gamma_e - 1}{\gamma_e}})\right] \quad \text{Eq.(12)}$$

The layout presented in Fig. 2 defines a particular Brayton cycle. Due to the relatively moderate maximum temperature, corresponding to $450\ ℃ < T_3 < 550\ ℃$, a net mechanical work $\dot{W}$ at the common turbocharger shaft is expected to be negligible. Instead, the mechanical work provided by the turbine can be enough to drive the compressor, allowing the air to flow inside the receiver tube without any external energy consumption. For that purpose, the turbocompressor freewheeling conditions must be satisfied, as stated in Eq. 13.

$$\dot{W} = \dot{W}_e\eta_m - \dot{W}_c = 0 \quad \text{Eq.(13)}$$

η_m is the mechanical efficiency of the turbocharger, assumed here as $\eta_m = 0.95$ (Heywood, 1988). Considering Eqs.6 to 13, for a given collector and solar irradiance, assuming turbocompressor efficiencies and π_c, the mass flow rate $\dot{m}_{\dot{w}=0}$ that satisfy Eq. 13 can be obtained. For a given solar power, a high mass flow rate lowers the inlet turbine temperature, according to Eq. 8, limiting the mechanical power extracted during the expansion $\dot{W}_e$. On the other hand, a high mass flow rate induces a larger pressure drop in the receiver tube, resulting in lower pressure at the turbine inlet, which also reduces the power $\dot{W}_e$. As consequence, for $\dot{m} > \dot{m}_{\dot{w}=0}$ external energy must be supplied to compensate for negative mechanical power $\dot{W} < 0$; for instance, using the auxiliary compressor *ac* in Fig.2. For $\dot{m} < \dot{m}_{\dot{w}=0}$ net mechanical power can be achieved. Alternatively, the turbine outlet pressure can be higher than atmospheric, so having $\pi_R > 1$, thus delivering air with a moderate over-pressure which can be beneficial for downstream utilisation. Although working with low $\dot{m}$ would increase $\dot{W}_e$, the risk of overheating the receiver tube arises. Commercial standard solar tubes present a maximum wall temperature limitation $T_{w,max}$

due to risk the degradation of the selective coating, and mechanical stress issues. Consequently, the outlet tube temperature is limited $T_3 < T_{w,max} - \Delta T_{w3}$, which turns into a minimum mass flow rate limit. During the turbocharger starting transient, an auxiliary compressor *ca* power $\dot{W}_{ca}$ is needed to circulate air before the steady-state operation point is reached (Fig. 2).

4. Results

As a preliminary study preceding a prototype design, a small scale Linear Fresnel collector LFC has been considered, having an effective reflective surface of length $L_t = 16$ m and a lateral aperture $W_a = 5$ m, equipped with a receiver based on 4 standard evacuated solar tubes with internal and external diameter $D = 66$ mm and $D_{ex} = 70$ mm respectively. Thermal losses correspond to an averaged heat transfer coefficient to the ambient $\bar{U}_l \sim 5$ W m^{-2} K^{-1}. The receiver tube length is considered equal to the reflector length.

Autonomous operation, achieved for $\dot{W} = 0$ and turbocharger in freewheeling, Eq.13, has been investigated under various conditions, as reported in Fig.3. Reaching autonomous operation is crucial to allows the system to work without any external energy consumption for air pumping, which is the aim of the proposed turbo-assisted air heating. The mass flow rate $\dot{m}_{\dot{w}=0}$ results from solving Eq.13 according to Eqs.8 to 12. Fig.3 shows $\dot{m}_{\dot{w}=0}$ versus net solar power input to the receiver tube per unit of collector area $G_{bn}\eta_{op,max}IAM$. In the numerical simulation, G_{bn}, $\eta_{op,max}$ and IAM have not been specified in order to hold general validity. Addressing proper values to them, allows to determine the specific working point, using Fig.3. The simulation of mass flow rate has carried out for several compression ratio $\pi_c = p_{2t}/p_{1t}$, in order to investigate its effect on the system behavior. On the other hand, constant isoentropic efficiencies of turbine and compressor $\eta_{ett} = \eta_{ctt} = 0.7$ have been considered, according to performances of automotive turbochargers (Heywood, 1988). In fact variation of η_{ett} and η_{ctt} with speed, pressure ratio and mass flow rate, determined by their efficiency maps, are out of the scope of this viability study. Null overpressure at the turbine outlet, $\pi_R = \frac{p_{4t}}{p_{atm}} = 1$ is assumed as reference case. As can be seen in Fig.3 the effect of π_c is not remarkable in the considered range $1.7 < \pi_c < 2.6$, which allow great flexibility during operation, according to turbocharger performances. Higher π_c have not been simulated according to the common turbocharger compression ratio range. On the other hand, increasing the compression ratio would translate into higher air temperature at the tube inlet, Eq. 7, reducing the operating ΔT across the receiver, hence requiring higher mass flow rate, which is a drawback in terms of pressure drops, Eq.2.

In addition to autonomous condition, the maximum tube temperature is a constrain. Maximum wall temperature T_{w3} occurs at the tube outlet where air temperature is maximum, according to Eq.5. In this point of the cycle, high air temperature T_3 is required for producing enough power at the turbine, in order to ensure autonomous condition, Eq.11. Wall temperature T_{w3} induced by T_3 under autonomous conditions must be below the receiver thermal limit $T_{w,max}$. For this reason T_{w3} corresponding to the system operating at $\dot{m}_{\dot{w}=0}$ is shown in Fig.3. Here the limit recommended by the manufacturers $T_{w,max} = 600$ °C is assumed. For presenting the results in a compact way, a non-dimensional temperature parameter is introduced $\Theta_{w3} = T_{w3}/T_{w3,max}$. In Fig.3 it can be observed that $\Theta_{w3} < 1$ for the considered π_c, except for $\pi_c = 2.6$, so that thermal limit is respected for almost all the working points.

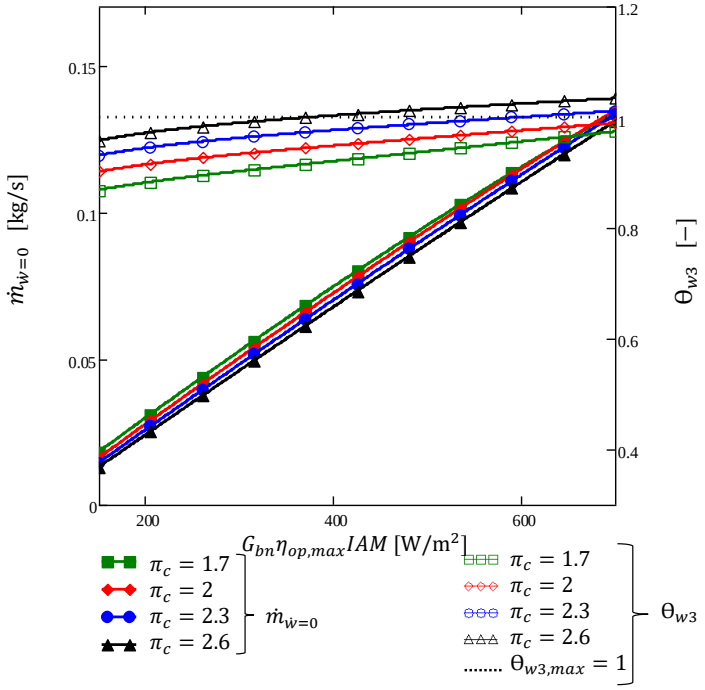

Figure 3. Characteristic mass flow rates and maximum wall temperature ratio vs. input power per unit of area

Fig. 4 shows the temperatures of the main representative points of the circuit versus the net solar power input to the receiver tube per unit of collector area, $G_{bn}\eta_{op,max}IAM$. They have been obtained with the system operating in autonomous condition, previously showed in Fig.3, hence for $\dot{m}_{\dot{w}=0}$ at an intermediate compression ratio $\pi_c = 2.2$. Air enters the receiver at temperature T_2, which results from the imposed compression ratio π_c, following Eq.7. Compressed air is heated up to T_3. End temperature T_3 depends on the input power $G_{bn}\eta_{op,max}IAM$ for a given collector area, as well as on the mass flow rate used. Receiver tube efficiency also affect the resulting T_3, Eq.8. It shows a smooth profile with the increasing $G_{bn}\eta_{op,max}IAM$, due to the growing mass flow rate applied according to autonomous operation requirements, shown in Fig.3. T_3 grows smoothly in order to allows turbine to compensate the increased pressure drop introduced by higher mass flow rates.

The maximum wall temperature T_{w3} is shown. Its growing trend with power input, shown in Fig.4, is due to the variation of heat flux transferred from the tube to the flow, which induce higher wall-to-flow temperature difference. On the other hand the increase of internal heat transfer due to higher mass flow rate used, slightly smooth the growing trend. The receiver tube outlet is lower than the considered thermal limit $T_{w3} < T_{w,max}$ within the wide range of power input values, confirming the viability of the concept and its flexibility.

The main output parameter is the temperature of delivered hot air, corresponding to turbine outlet, T_4. Fig. 4 shows that its value is almost steady, holding $T_4 > 350$ ºC, which is useful temperature for many industrial process needs, according to the aim of the present technology assessment.

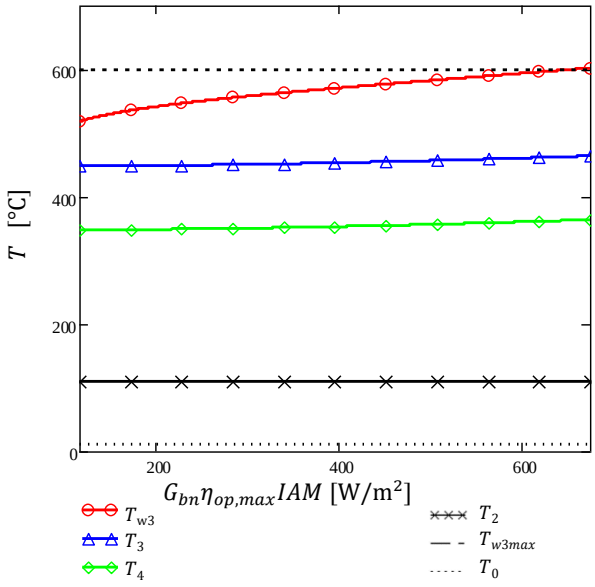

Figure 4. Temperatures vs. input power per unit of area for $\dot{m}_{\dot{w}=0}$

Fig.5 displays the mechanical power provided by the turbine $\dot{W}_e$ as well as the compressor mechanical power consumption, for the system working in autonomous condition with $\dot{m}_{\dot{w}=0}$. The simulation has been carried out across a wide the range of net solar power input per unit of collector area $G_{bn}\eta_{op,max}IAM$. Solar power gathered by the receiver tube $\dot{Q}_s = L_a L_t G_{bn}\eta_{op,max}IAM$ is also shown. As a consequence of thermal losses to ambient, Eq.8, it holds that the thermal power $\dot{Q}_d < \dot{Q}_s$ is delivered to air and is available for user's thermal process. According to Eq.8, the thermal efficiency of the collector increases with $G_{bn}\eta_{op,max}IAM$ as confirmed in Fig.6. The final output of the system is the power delivered to the produced hot air flow, at the turbine exit $\dot{Q}_d = \dot{m}_{\dot{w}=0}(T_{4t}c_{p4} - T_{atm}c_{p,atm})$, Fig 5. The system is working in autonomous condition: the turbine is able to produce the mechanical power needed by the compressor $\dot{W}_c\eta_m$ as shown in Fig.5.

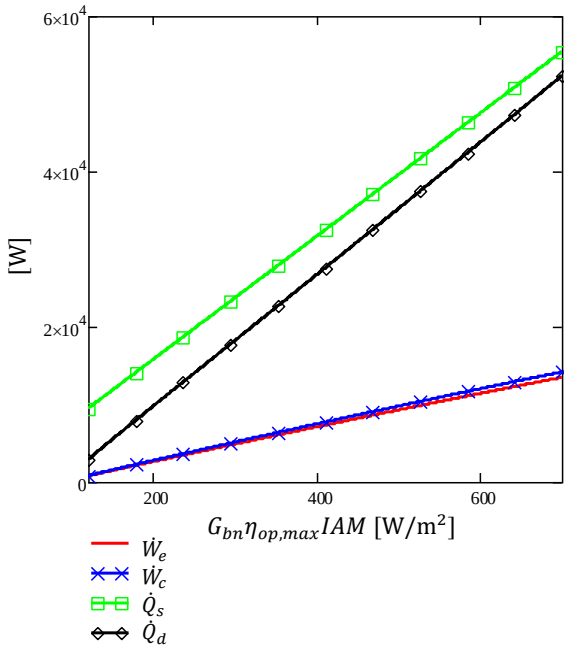

Figure 5. Powers vs. input power per unit of area for $\dot{m}_{\dot{w}=0}$

As shown in Fig.3, working with $\dot{m}_{\dot{w}=0}$ ensures the turbocharger to work in freewheeling. Moreover working with $\dot{m}_{\dot{w}=0}$ keep the maximum wall temperature below the thermal limit $T_{w,max}$. Moreover, for given values of input power $G_{bn}\eta_{op,max}IAM$, compression ratio π_c and efficiencies $\eta_{ett} = \eta_{ctt}$, this is not the only possible working point. In fact, previous analysis has been carried out considering the turbine outlet at atmospheric pressure, hence with $\pi_R = 1$. As mentioned above, according to operating constrains, producing hot air at certain slightly overpressure than ambient would be beneficial for the potential user, either for pumping hot air flow up to the thermal process location, and for driving the thermal process itself, if required.

In order to explore this possibility $\pi_R > 1$ must be considered in the numerical simulations. Reducing the mass flow rate with respect to $\dot{m}_{\dot{w}=0}$ induces a frictional pressure drop reduction. As result, an increase of inlet pressure at the turbine is expected, which is beneficial on the turbine mechanical power generation, at constant η_{ett}. The excess of net power at the turbocharger shaft could be extracted, for instance coupling the turbine with an electricity generator, but this seems not convenient in our case. Instead, the expansion pressure ratio can be reduced so that air exits the turbine at higher pressure $p_{4t} > p_{atm}$. This means reaching autonomous conditions using $\pi_R = p_{4t}/p_{atm} > 1$. As a drawback, smaller mass flow rate leads to lower internal heat transfer, which is controlled by Reynolds number as in Eq.4. As consequence, the maximum wall temperature increases and the risk of tube overheating arises. The minimum mass flow rate allowed is the one which gives $T_{w3} = T_{w,max}$.

Fig.6 depicts $\Delta p_R = p_{4t} - p_{atm}$ for several turbocharger efficiencies $\eta_{TC} = \eta_{ctt}\eta_{ett}\eta_m$ (Heywood, 1988). High performing turbochargers allow higher delivery overpressure, as expected. On the other hand, higher Δp_R are possible when working with low solar power, due to the lower mass flow rate required and lower internal pressure drops, ceteris paribus assumption.

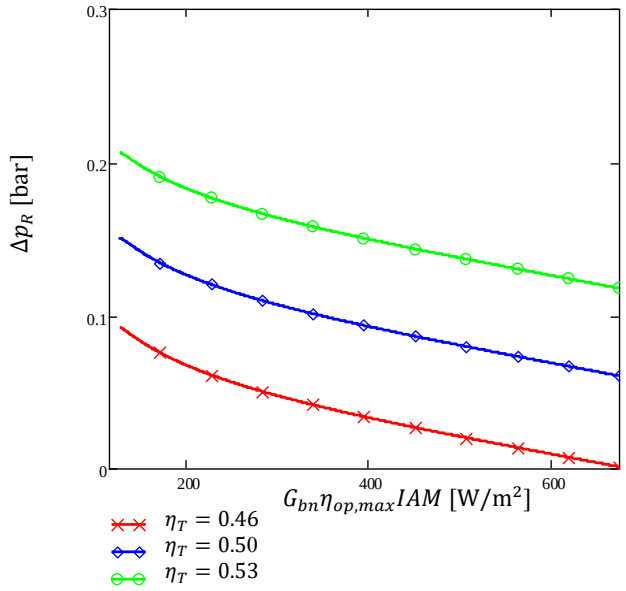

Figure 6. Delivery overpressure vs input power per unit of area for several turbocharger efficiencies

5. Conclusions

Directly heating air using concentrating collector either parabolic trough or linear Fresnel types reduces the complexity and the initial and operating costs of solar plant by eliminating the liquid HTF as well as its heat exchanger.

Using ambient air as HTF in an open circuit layout is attractive for driving the thermal process with intensive hot air consumption. Due to air physical properties, the pumping power consumption for large installation can be high, and the moderate internal heat transfer of air can lead to the receiver tube overheating.

The innovative layout presented uses compressed air to reduce the pressure drops and pumping consumption. Thanks to a Brayton cycle configuration, compression power is recovered by a turbine driven by solar energy enabling the system to run without any external mechanical energy consumption, delivering to user hot air up to 350°C.

The study performed supports the viability of this innovative direct air heating system proposed. The results indicate that a small installation is feasible, although is performances are limited by the moderate turbocharger efficiencies of very small size. Larger sizes promise higher efficiencies, enabling very favourable performances of the layout here scrutinized.

6. Acknowledgments

The partial funding of the research project "*Producción directa de aire a alta temperatura y a presión turboalimentada en colectores solares de concentración*" BOCM (10/01/2018), Orden 4586/2017, december 13th, project IND2017/AMB7769, from CAM "Comunidad de Madrid", it is greatly appreciated.

7. List of Symbols

Latin	
A_a	Aperture collector area
c_p	Specific heat capacity
D	Diameter
f	Friction factor
F'	Collector efficiency factor [-]
F_R	Heat removal factor
G_{bn}	Normal direct irradiance
G_{bT}	Direct irradiance on tilted surface
h	Heat transfer coefficient
k	Thermal conductivity
L_t	Tube Length
$\dot{m}$	Mass flow rate
$\dot{m}_{\dot{w}=0}$	Autonomous operation mass flow rate
$\dot{Q}_d$	Delivery power
$\dot{Q}_s$	Solar power to receiver tube
$\dot{Q}_u$	Useful solar power to air flow
$\dot{q}_u$	Useful heat flux to air flow
v	Mean velocity
p	pressure
P	Perimeter
Pr	Prandtl Number
Re	Reynolds number
T	Temperature
$\bar{U}_l$	Heat losses coefficient
W_a	Aperture Width
$\dot{W}_p$	Pumping Power
Greek	
Δ	Variation
Δp	Pressure drop
γ	Isentropic exponent
ρ	Density
μ	viscosity
η_{ctt}	Compressor efficiency total to total
η_{ett}	Turbine efficiency total to total
η_m	Turbocharger mechanical efficiency
η_{op}	Optical efficiency
π_c	Compression ratio
π_R	Residual overpressure ratio
Θ_{w3max}	Maximum wall temperature ratio
Subscripts	
a	air
ac	Auxiliary compressor
amb	ambient
atm	atmosferic
c	compressor
e	turbine
ex	external
in	Inlet
L	longitudinal

m	Average value
max	Maximum
n	Connection tube
r	Receiver tube
R	Residual
t	Total, tube
T	Trasversal
ou	outlet
w	Wall, tube surface
Acronyms	
IAM	Incident Angle Modifier
LFC	Linear Fresnel Collector
PTC	Parabolic trough Collector
HTF	Heat Transfer Fluid
HX	Heat Exchanger

8. References

Balje, O. (1981). *Turbomachines.* New York: John Wiley.

Bellos, E., Tzivanidis, C., & Antonopoulos, K. A. (2017). Parametric analysis and optimization of a solar assisted gas turbine. *Energy Conversion and Management, 137*, 151-165. doi:10.1016/j.enconman.2017.02.042

Blasius, H. P. (1913). Das Aehnlichkeitsgesetz bei Reibungsvorgangen in Flüssigkeiten. *Forschungsheft, 131*, 1-41.

Cinocca, A., Cipollone, R., Carapellucci, R., Iampieri, V., & Mattia, R. (2018). CSP-PT gas plant using air as Heat Transfer Fluid with a packed bed storage section. *Energy Procedia. 0*, pp. 0-0. Elsevier. Retrieved 09 29, 2018, from https://www.researchgate.net/publication/327728983

Duffie, J. A., & Beckman, W. A. (1991). *Solar Engineering of Thermal Processes.* Hoboken, New Jersey, USA: John Wiley & Sons.

European Comission. (2018, 10 02). Heating and cooling. Brussels, Belgium, Belgium. Retrieved from https://ec.europa.eu/energy/en/topics/energy-efficiency/heating-and-cooling

Farjana, S., Huda, N., Parvez Mahmud, M., & Saidur, R. (2018). Solar process heat in industrial systems – A global review. *Renewable and Sustainable Energy Reviews, 82*(3), 2270-2286. doi:https://doi.org/10.1016/j.rser.2017.08.065

Heywood, J. (1988). *Internal Combustion Engine Fundamentals.* New York: McGraw-Hill.

IRENA. (2015). *Solar heat for industrial processes - Technology Brief. IEA-ETSAP and IRENA Technology Brief E21.* International Renewable Energy Agency, Energy Technology Systems Analysis Programme. International Renewable Energy Agency. Retrieved 09 29, 2018, from iea-etsap.org/web/Supply.asp

Lecuona-Neumann, A. (2016, 1 21). *Spain Patent No. P201630068.*

Wilson, D., & Korakianitis, T. (1998). *The design of high-efficiency turbomachinery and gas turbines* (2 ed.). Cambridge, Massachusetts, USA: MIT Press.

Zhu, G., Wendelin, T., Wagner, M., & Kutscher, C. (2014). History, current state, and future of linear Fresnel concentrating solar collectors. *Solar Energy, 103*, 639-652. doi:https://doi.org/10.1016/j.solener.2013.05.021